Triphasic Force Dependence of E-Selectin/Ligand Dissociation Governs Cell Rolling under Flow

Annica M. Wayman,[†] Wei Chen,[†‡] Rodger P. McEver,[§¶] and Cheng Zhu[†‡*]

[†]Woodruff School of Mechanical Engineering, [‡]Coulter Department of Biomedical Engineering, Georgia Institute of Technology, Atlanta, Georgia; [§]Cardiovascular Biology Research Program, Oklahoma Medical Research Foundation, and [¶]Department of Biochemistry and Molecular Biology, Oklahoma Center for Medical Glycobiology, University of Oklahoma Health Science Center, Oklahoma City, Oklahoma

ABSTRACT During inflammation, flowing leukocytes tether to and roll on vascular surfaces through the association and dissociation of selectin/ligand bonds. The interactions of P- and L- selectins with their respective ligands exhibit catch-slip bonds, such that increasing force initially prolongs and then shortens bond lifetimes. In addition, catch-slip bonds have been shown to govern L-selectin-mediated cell rolling. Using a flow chamber and biomembrane force probe, we show a triphasic force dependence of E-selectin/ligand dissociation that initially behaves as slip bonds, then transitions to catch bonds, and finally transitions again to slip bonds as the force increases. These transitions govern the velocities of neutrophils, HL-60 cells, and Colo-205 cells rolling on E-selectin, as evidenced by the fact that their velocities exhibited a triphasic force dependence that inversely matched the triphasic lifetime-force relationship. At low forces, slip bonds may also precede catch bonds for interactions of P- and L-selectin with their ligands.

INTRODUCTION

During inflammation, selectins play a primary role in leukocyte trafficking by mediating tethering to and rolling on vascular surfaces (1–3). The selectin family is comprised of P-, E-, and L-selectin. All selectins have an N-terminal C-type lectin domain that is followed by an epidermal growth factor (EGF)-like domain, a series of consensus repeats, a transmembrane domain, and a cytoplasmic tail (4).

Although the ligands specific for each of the three selectins vary, a common glycan determinant on all selectin ligands is sialyl Lewis x (sLe^x). This carbohydrate structure contains a sialic acid and fucose component (5–8). The best-characterized sLe^x-containing ligand is the homodimeric mucin P-selectin glycoprotein ligand-1 (PSGL-1), which binds to all three selectins. PSGL-1 is constitutively expressed on the microvillous tips of leukocytes, extending 50–60 nm from the surface (9).

Selectin-ligand binding depends on the unique properties of each interaction pair. The formation and breakage of selectin-ligand bonds are characterized by the kinetic parameters of the association and dissociation rates, respectively. Bell (10) proposed that in first-order dissociation kinetics, k_{off} increases exponentially with increasing bond force, which is known as a slip bond. However, using atomic force microscopy (AFM) and flow chamber experiments, Marshall et al. (11) observed that interactions of dimeric P-selectin with dimeric and monomeric PSGL-1 formed catch bonds at forces ranging from 5 to 10 and 20 pN, respectively, and at higher forces the catch bonds transitioned to slip bonds. L-selectin was also observed to form catch bonds with PSGL-1 at forces ranging from 5 to 75 pN, which transitioned to slip bonds at higher forces (12). Catch bonds between L-selectin and its ligands govern flow-enhanced adhesion, such that rolling becomes slower and more regular as shear increases above a threshold. Once an optimal shear is achieved, the transition to slip bonds causes cells to roll faster and more irregularly as shear increases further (13).

The zero-force off-rates (k°_{off}) obtained by extrapolating from the catch-bond regime of the respective P- and L-selectin off-rate versus force curves are significantly higher than the values seen in other studies. In micropipette adhesion frequency experiments, k°_{off} was determined to be 0.55 s^{-1} (14) and 0.9 s^{-1} (15) for P-selectin dissociating from HL-60 cell PSGL-1. Using a thermal fluctuation assay with a biomembrane force probe (BFP), Chen et al. (16) determined the k°_{off} for PSGL-1 dissociating from P- and L-selectin to be 2.68 and 10.2 s^{-1}, respectively. Using surface plasma resonance (SPR), Mehta et al. (17) obtained a value of 1.4 $\pm$ 0.1 s^{-1} for the off-rate of P-selectin/PSGL-1 dissociation. Using SPR, Nicholson et al. (18) estimated a $k^\circ_{off} \geq 10$ s^{-1} for L-selectin dissociating from glycosylation-dependent cell adhesion molecule-1 (GlyCAM-1). All of these measurements are substantially lower than the corresponding values estimated from the zero-force extrapolation of the respective P- and L-selectin catch-bond curves. Therefore, it remains to be determined how dissociation in the catch-bond region integrates with k°_{off}.

Studies of the force-dependent dissociation kinetics of E-selectin may provide insight into the zero-force off-rate for P- and L-selectin. A catch-slip bond transition similar to that observed for P- and L-selectin would be expected for E-selectin because of the similarity in structure and function of the three selectins. This catch-slip bond transition

Submitted March 22, 2010, and accepted for publication May 19, 2010.

*Correspondence: cheng.zhu@bme.gatech.edu

Annica M. Wayman's present address is BD, Franklin Lakes, New Jersey.

Editor: Lewis H. Romer.

0006-3495/10/08/1166/9 $2.00

doi: 10.1016/j.bpj.2010.05.040

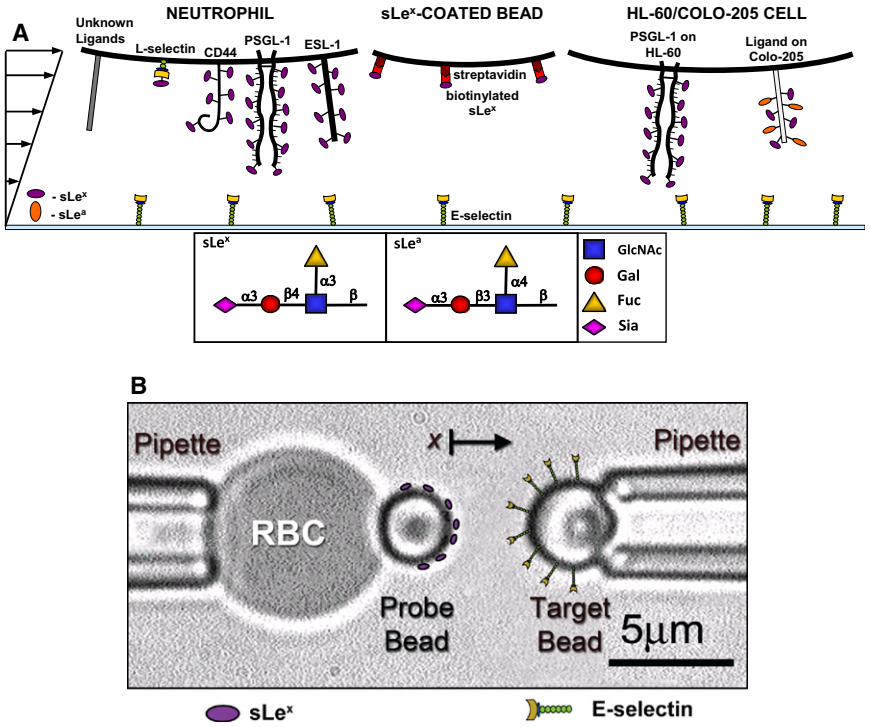

FIGURE 1 Schematics of the flow chamber (*A*) and BFP (*B*) experiments. Shown are the cells, chamber floor, and beads, as well as the interacting molecules that are expressed or coated on the surfaces.

might occur in a different force range. A shift of the catch-slip bond transition to a higher range of forces for E-selectin than for P- and L-selectin may allow observation of the dissociation kinetics at forces lower than the catch-bond regime. Indeed, preliminary micropipette measurements of force-dependent lifetimes of E-selectin interacting with Colo-205 cells suggest that a slip-bond regime precedes the catch-slip bond regime with a zero-force extrapolation in agreement with that measured using the adhesion frequency assay (19).

The structural and functional similarities of the three selectins suggest that catch bonds may also regulate flow-enhanced rolling adhesion of P- and E-selectin. Although the shear threshold is more pronounced for L-selectin, correlation of the off-rate with the rolling velocity with increasing force for P- and E-selectin would also be expected. This would relate catch bonds to the rolling velocity for all three selectins. Here, we use the results of flow chamber and BFP experiments to show the triphasic force dependence of E-selectin/ligand dissociation and the correlation of this off-rate versus force trend to the force-dependent rolling velocities of neutrophils, HL-60 cells and Colo-205 cells on E-selectin substrates.

MATERIALS AND METHODS

Cells and molecules

Human soluble E-selectin (sEs) (20) and the anti-E-selectin monoclonal antibody (mAb) ES1 (21) were used as previously described. Fluorescently conjugated anti-sLe^x mAb HECA-452 was obtained from BD Pharmingen (San Diego, CA). Multivalent biotinylated sLe^x was obtained from GlycoTech (Gaithersburg, MD).

Human neutrophils were freshly isolated from healthy donors according to a protocol approved by Georgia Institute of Technology's institutional review board. For this procedure we used Dextran 70 (BBraun, Irvine, CA) followed by separation from the lymphocytes using Ficoll-Hypaque (Histopaque 77; Sigma Diagnostics, St. Louis, MO) as described by Zimmerman et al. (22). Neutrophils were suspended in Hanks balanced salt solution with 0.5% human serum albumin (Sigma) at 0.5–1.0 $\times$ 10^6 cells/mL and used within 8 h.

The human promyelocytic leukemic cell line HL-60 and human colon adenocarcinoma cell line Colo-205 were obtained from the American Type Culture Collection (Rockville, MD). Both were cultured using RPMI 1640 media (Cellgro, Herndon, VA) supplemented with 10% fetal calf serum, 1% L-glutamine and 1% penicillin-streptomycin (Sigma).

Fresh human red blood cells (RBCs) were isolated from a blood drop via finger prick according to a protocol approved by the Georgia Institute of Technology's institutional review board. The RBCs were then biotinylated as described previously (16). Briefly, fresh human RBCs were resuspended in carbonate/bicarbonate buffer (pH = 8.4), incubated with biotin-PEG3500-NHS (Nektar, San Carlos, CA) for 30 min at room temperature, and washed with and resuspended in Hepes buffer (pH = 7.4, 300 mOsm) (23).

Coupling sLe^x and E-selectin on microsphere and flow chamber surfaces

For flow chamber experiments, streptavidin-coated 6-μm-diameter beads (Polyscience, Warrington, PA) were coupled with multivalent biotinylated sLe^x (GlycoTech, Gaithersburg, MD) by mixing at 4°C for 1 h. Coupling of sLe^x was confirmed by flow cytometry with the anti-sLe^x mAb HECA-452.

The sEs was directly adsorbed on coverglasses used for the flow chamber floor (Fig. 1 *A*) by incubation for >2 h at room temperature. The coverglasses were cleaned with 70% sulfuric acid and 30% diluted hydrogen

peroxide before they were coated with the sEs. To block nonspecific adhesion, 1% bovine serum albumin (BSA) was applied to the coverglass after incubation with sEs, followed by incubation with 0.5% Tween 20 (Sigma) for bead experiments (24).

For BFP experiments (16,23), borosilicate glass beads (Duke Scientific, Palo Alto, CA) were cleaned with a mixture of ammonium hydroxide, hydrogen peroxide, and water at boiling temperature. The beads were covalently coupled with mercapto-propyl-trimethoxy silane (United Chemical Technologies, Bristol, PA). One set of silanized beads was covalently linked with E-selectin, which was precoupled covalently with maleimide-PEG3500-NHS. Another set of beads was covalently linked with a mixture of streptavidin-maleimide and hydrolyzed maleimide-PEG3500-NHS (Nektar). Biotinylated sLe^x was incubated with the streptavidinylated beads.

Site density determination

A radioimmunoassay was used to measure the site densities of E-selectin absorbed on coverglasses. Iodination of the anti-E-selectin mAb ES1 was performed as described previously (25). Circular coverglasses similar to those used in the flow chamber were coated with various concentrations of sEs. The binding of ^{125}I-labeled ES1 to sEs was measured to determine the available binding sites of sEs on the surfaces.

Flow chamber assays

A parallel plate flow chamber was constructed by using two rectangular Lexan pieces of equal thickness to enclose a rigid gasket and protein-coated coverglass. Cells or beads were perfused through the flow chamber (Fig. 1 *A*) using a syringe pump, observed using an inverted microscope, and recorded at 30 frames per second (fps) using a CCD analog camera (AutomatiCam A106, World Video Sales, Boyertown, PA). Video segments were acquired with an A/D converter (Pinnacle Systems, Mountain View, CA) and the experiments were then analyzed using frame-by-frame playback.

Tethering frequency was measured by dividing the number of cells that initially tethered to the surface by the total number of cells that were sufficiently close to the surface and capable of tethering within the first minute of the experiment. The average rolling velocity was measured by dividing the rolling distance by the travel time (5–10 s). The transient tether lifetimes of cells or beads were quantified by counting the number of frames during which the cell/bead paused. For each wall shear stress under each condition, 50–100 transient tether lifetimes were measured. Most experiments were repeated at least once at each condition.

The tether forces for the cells and beads were estimated as described previously (26,27) assuming similar tether properties between the three selectin types. Briefly, the lever arm of the tethered neutrophils or beads was measured by means of flow reversal and used to derive the tether angle (27). With the tether angle, the tether force can be determined using the exact solution of the Stokes equation for neutrally buoyant spheres (28), resulting in the relationship between the shear stress on the cell or bead and the tether force. By assuming that the tether properties of HL-60 cells and Colo-205 cells are similar to those of neutrophils, we were able to use the dimensionless parameter, $F_{t\infty}/(r^2\mu\dot{\gamma})$ determined previously (13) (where $F_{t\infty}$ represents the maximum tether force that develops when the cell completely stops, r is the radius, μ is viscosity, and $\dot{\gamma}$ is the shear rate), to find the ratio of the tether force to the wall shear stress for HL-60 and Colo-205 cells.

Single-bond lifetime measurements obtained with a BFP

The BFP apparatus has been described previously (16,23). Briefly, an ultrasensitive force probe was assembled by attaching a streptavidinylated bead bearing biotinylated sLe^x to the apex of a biotinylated RBC that was aspirated by a micropipette (Fig. 1 *B*, *left*). The aspiration pressure was set by a manometer with micrometer precision. An E-selectin-bearing target bead aspirated by another micropipette was driven by a piezoelectric translator with subnanometer precision via a capacitive sensor feedback control (Fig. 1 *B*, *right*). The two beads were aligned and observed under an inverted microscope through two cameras. One had a standard video rate of 30 fps to provide real-time images. The other had a high speed (1600 fps) when the images were limited to a 24-line strip across the bead, which allowed a custom image analysis software to track the bead's position with a spatial precision of 5 nm (29). The BFP spring constant was determined from the suction pressure and the radii of the pipette, the spherical portion of the RBC, and the contact area between the probe and the RBC (16,30). The spring constant was set at 0.3 pN/nm.

Analysis of bond lifetimes

Bond lifetimes were measured at a constant wall shear stress or force, pooled, and analyzed by a model for the first-order kinetics of irreversible dissociation of single bonds:

$$p(t) = \exp\left(-k_{\text{off}}t\right) \tag{1}$$

where p is the probability for a bond formed at time 0 to remain bound at time t, and k_{off} is the off-rate. Taking the natural log of p linearizes the exponential distribution so that the negative slope of the ln(No. of events with a lifetime $> t$) versus t plot equals k_{off} (see Supporting Material). It follows from Eq. 1 that the average lifetime $\langle t\rangle = \int_0^\infty td(1-p) = 1/k_{\text{off}}$ and the standard deviation (SD) of lifetime $\sigma(t) = \int_0^\infty (t-\langle t\rangle)^2 d(1-p) = 1/k_{\text{off}}$. Therefore, individual lifetimes measured at each force bin are presented as the average and SD of lifetimes as well as the -1/slope of the lifetime distribution in the semi-log plot.

Statistical analysis

To test whether the changes in the trends of the force-dependent tether lifetime and rolling velocity data were statistically significant, the respective slopes of the monotonically increasing and decreasing phases adjacent to each other in one curve were compared. Linear regression was used to obtain the slopes and other statistical parameters for each line segment. A t-statistic can be calculated to test the hypothesis of equal slopes by using Eq. 2:

$$t = \frac{b_1 - b_2}{S_{b1-b2}} \tag{2}$$

where b_1 and b_2 are the slopes of the two line segments, and

$$S_{b1-b2} = \sqrt{\left(\frac{\left(S^2_{Y\cdot X}\right)_P}{\left(\sum x^2\right)_1} + \frac{\left(S^2_{Y\cdot X}\right)_P}{\left(\sum x^2\right)_2}\right)} \tag{3}$$

where $(s^2_{Y\cdot X})_P$ is the pooled residual mean squared, which is found by dividing the sum of the residual sum of squares for both linear curves by the sum of the residual degrees of freedom for the two lines. The P-values can then be obtained by using a two-tailed t-distribution table in which the degrees of freedom equal the sum of the residual degrees of freedom (31).

RESULTS

E-selectin/ligand interaction is specific and calcium-dependent

To ensure that our flow chamber experiments measured specific E-selectin/ligand interaction, we measured the

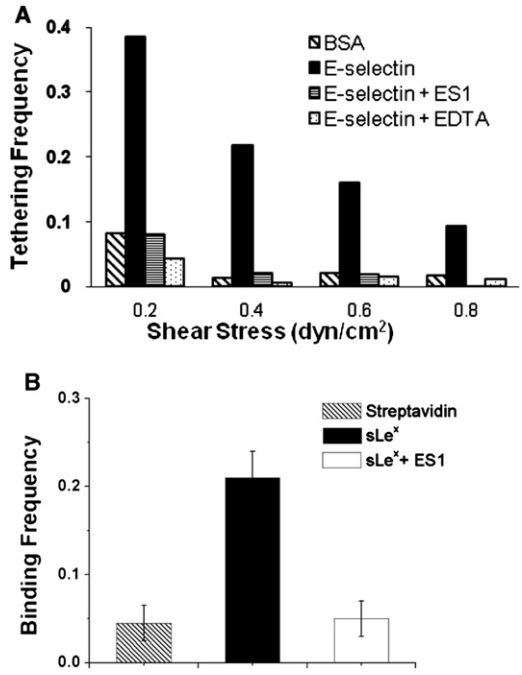

FIGURE 2 Specificity of E-selectin-mediated adhesion. (*A*) The frequencies of flowing neutrophils tethering to a chamber floor coated with BSA or 5 μm^{-2} E-selectin in the absence or presence of 20 μg/mL of an anti-E-selectin blocking antibody (ES1) or 5 mM EDTA measured in a range of wall shear stresses. Representative data of five or more experiments. (*B*) The binding frequencies of E-selectin-coated beads to beads bearing streptavidin or sLe^x in the absence or presence of ES1. Data are presented as the mean $\pm$ SE of three pairs of beads.

tethering frequency of neutrophils to 5 μm^{-2} E-selectin substrates at wall shear stresses of 0.2, 0.4, 0.6, and 0.8 dyn/cm^2 and compared the results with results obtained under various control conditions (Fig. 2 *A*). Not coating E-selectin on the substrate (BSA only) or adding anti-E-selectin antibody (ES1) or the divalent cation chelator (EDTA) to E-selectin substrates greatly reduced tether frequencies. Similar results were found for tethering of sLe^x-coated beads and HL-60 cells (data not shown). These results confirmed that the observed adhesive events were mediated by specific, calcium-dependent binding of E-selectin to its ligands.

The BFP also measured specific E-selectin/sLe^x interactions because, compared to the experimental condition with sLe^x-coated probe beads (sLe^x), not coating with sLe^x (streptavidin only) or adding the anti-E-selectin antibody (ES1) substantially lowered binding frequencies with the E-selectin-coated target beads (Fig. 2 *B*).

E-selectin/ligand dissociation displays triphasic force dependence

To test the hypothesis that E-selectin/ligand interactions behave as catch bonds in a certain force range, we used a flow chamber to measure the lifetimes of transient tethering events of neutrophils to E-selectin immobilized at a density of 5 μm^{-2} under constant wall shear stresses ranging from 0.05 to 0.8 dyn/cm^2. Data were plotted as dissociation curves, ln(# of events with a lifetime $\geq t$) versus t, for each shear stress (see Fig. S1), which generated straight lines consistent with first-order kinetics. It follows that the negative slope (-1/slope) of the linear fit to the data equals the off-rate (k_{off}) of E-selectin/ligand dissociation. This negative slope also equals the reciprocal average tether lifetime ($1/<t>$) and reciprocal SD ($1/\sigma(t)$) of lifetimes at each wall shear stress. Two or three independent experiments were done for each shear stress, with the exception of 0.15 dyn/cm^2, for which only one experiment was conducted.

The force dependence of the three tether lifetimes metrics are shown in Fig. 3 *A*, where -1/slope, $<t>$, and $\sigma(t)$ are plotted versus the wall shear stress (first x axis) and tether force (second x axis) for neutrophil ligands dissociating from E-selectin. At high wall shear stresses (>0.5 dyn/cm^2), the lifetimes decreased as the shear increased. These represent the slip bonds most commonly seen in selectin dissociation studies (26). At intermediate wall shear stresses (0.25–0.5 dyn/cm^2), however, the lifetimes increased as the shear increased, which is a hallmark of catch bonds. At low wall shear stresses (<0.25 dyn/cm^2), the lifetimes returned to slip-bond behavior. Thus, the tether lifetimes of neutrophil ligands with E-selectin exhibit a triphasic behavior that changes from slip bonds to catch bonds and returns to slip bonds as force increases.

Neutrophils express several E-selectin ligands, including PSGL-1, CD44, and E-selectin ligand 1 (ESL-1), as shown in Fig. 1 *A*, which raised the question as to whether the triphasic lifetime versus force curves in Fig. 3 *A* were caused by mixed populations of E-selectin/ligand bonds. Because all of these ligands bear sLe^x-capped glycans (9), we measured the lifetimes of sLe^x-coated 6-μm-diameter beads tethering to 30 μm^{-2} E-selectin. For this cell-free system, a higher density of E-selectin was necessary to obtain a sufficiently high tether frequency for lifetime measurements. Despite the higher coating density of E-selectin, the interactions were transient and specific (data not shown).

For each shear stress, two to four independent experiments were performed. The dissociation curves were linear, indicating that dissociation followed first-order kinetics (see Fig. S2). The average and SE of the three tether lifetime metrics are plotted versus wall shear stress and tether force in Fig. 3 *B*. The lifetimes of the sLe^x-coated beads binding to E-selectin were shorter than those of the neutrophils. Despite the shorter lifetimes, however, the dissociation of the E-selectin/sLe^x interaction exhibited a triphasic dependence on force similar to that of the E-selectin/neutrophil ligand interactions, with the regime transitions occurring at similar force ranges.

To test whether the changes from slip bonds to catch bonds and back to slip bonds were statistically significant, we compared the trends of the data in the two neighboring

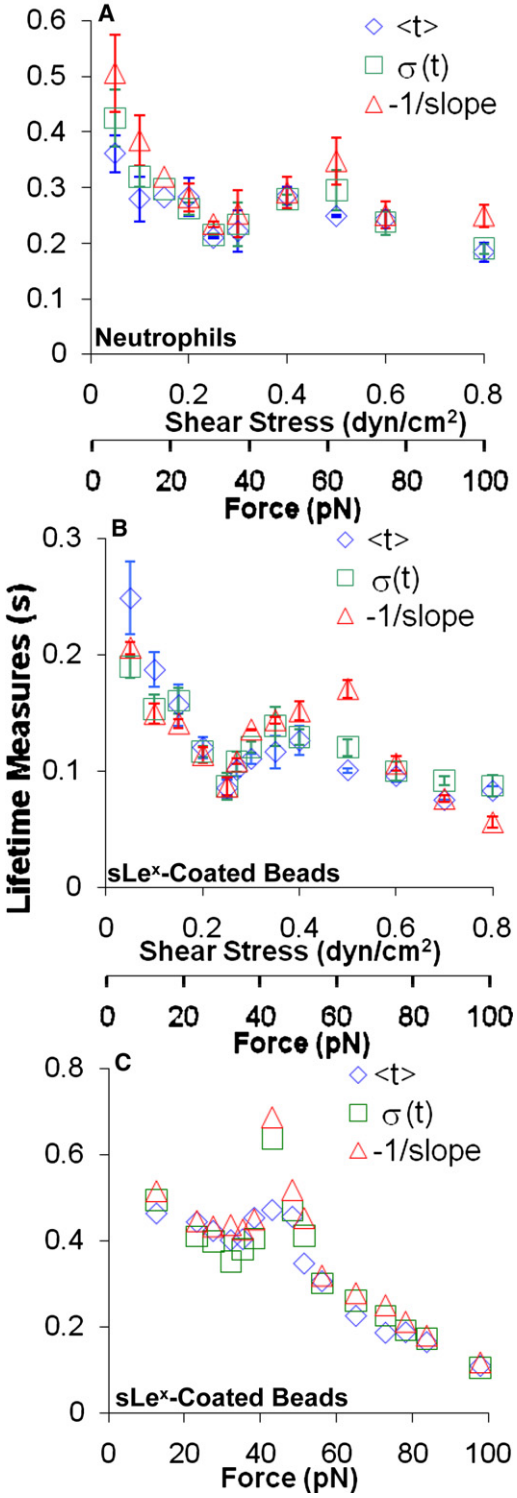

FIGURE 3 Triphasic force dependence of bond lifetimes. (*A* and *B*) Flow chamber data. Lifetimes of neutrophils (*A*) or 6-μm-diameter beads bearing sLe^x (*B*) transiently tethered to flow chamber floors coated with 5 or 30 μm^{-2} E-selectin, respectively, at a range of wall shear stresses. Data are presented as the mean ± SE of two to four experiments. (*C*) BFP data. The lifetimes of E-selectin/sLe^x bonds at a range of forces are shown. Three metrics of lifetimes were measured at each force: average, SD, and reciprocal slope of the ln(# of events with a lifetime $> t$) versus t plots of several tens of lifetimes (see Fig. S1, Fig. S2, and Fig. S3).

TABLE 1 *P*-Values used to test the statistical significance of the differences in the slopes of two neighboring phases of the triphasic curve for the E-selectin/neutrophil ligand dissociation

P-Value	$<t>$	-1/slope	$\sigma(t)$
Slip$_1$/Catch	0.018	0.0003	0.0005
Catch/Slip$_2$	0.0043	0.04	0.0048

phases of each transition. This comparison is more appropriate than comparing the tether lifetimes of neighboring points because small changes in the wall shear stresses cause only subtle changes in the tether lifetimes, and data in neighboring points along the same trend line are correlated. For each lifetime metric, each regime of the triphasic curve followed a statistically significant monotonically increasing or decreasing line with 95–99% confidence, except for the second slip-bond regime at high shear stresses, where fewer tether lifetimes were measured. Therefore, we compared the slopes of each regime that were obtained through linear regression by calculating the *t*-statistics to obtain the P-values (31). The two slopes for each transition, the slip region at the very low shear stresses transitioning to the catch regime (Slip$_1$/Catch), and the catch regime transitioning to the slip region at high shear stresses (Catch/Slip$_2$), proved to be statistically different, with $P < 0.05$ in every comparison for all three lifetime metrics for both cases of E-selectin/neutrophil ligands (Table 1) and E-selectin/sLe^x (Table 2) dissociation. Thus, the slip-catch-slip bond trend of the E-selectin/ligand interactions is statistically significant.

To further demonstrate the triphasic slip-catch-slip bond transition of the E-selectin/ligand interactions, we used the BFP to directly measure the force-dependent E-selectin/sLe^x bond lifetimes at a single-bond level (Fig. 1 *B*), which also exhibited first-order dissociation kinetics (see Fig. S3). It is evident from Fig. 3 *C* that increasing force first shortened the bond lifetimes (slip bonds), then prolonged the bond lifetimes in the 30–40 pN force range (catch bonds), and finally shortened the bond lifetimes again beyond 40 pN (slip bonds). Thus, the slip-catch-slip bond transition of E-selectin/sLe^x interaction was also observed in the BFP experiments, confirming the observations in the flow chamber experiments.

Triphasic shear-dependent rolling velocity of cells on E-selectin

Catch bonds govern the counterintuitive, flow-enhanced rolling adhesion mediated by interactions between L-selectin and ligands (13) and between platelet glycoprotein Ibα

TABLE 2 *P*-Values used to test the statistical significance of the differences in the slopes of two neighboring phases of the triphasic curve for the E-selectin/sLe^x dissociation

P-Value	$<t>$	-1/slope	$\sigma(t)$
Slip$_1$/Catch	<0.0001	0.0001	0.0014
Catch/Slip$_2$	0.0025	0.0004	0.0039

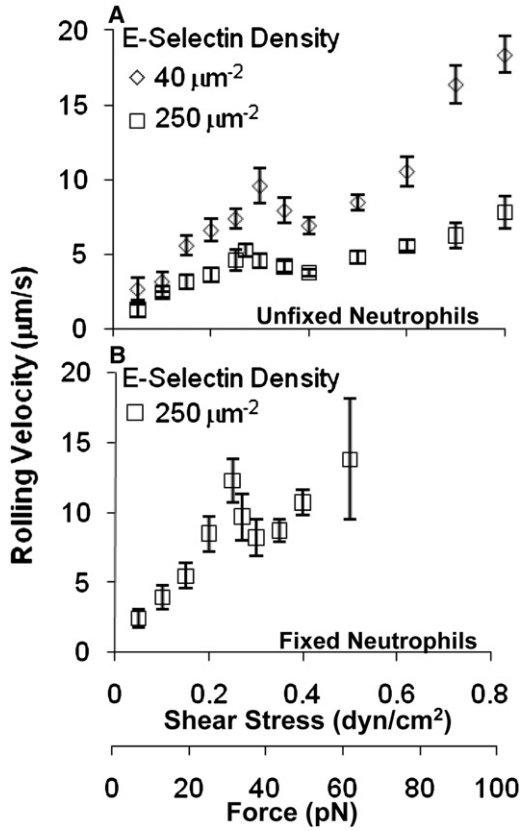

FIGURE 4 Triphasic shear stress dependence of neutrophil rolling velocities. (*A* and *B*) The velocities of unfixed (*A*) and fixed (*B*) neutrophils rolling on E-selectin at indicated site densities at various shear stresses. Data are presented as velocity mean ± SE of up to 30 cells.

(GPIbα) and von Willebrand factor (VWF) (32). To test the hypothesis that the slip-catch-slip bonds of E-selectin/ligand interactions also govern the rolling behavior of cells supported by these interactions, we measured the average velocities of 15–30 neutrophils rolling on 40 and 250 μm^{-2} E-selectin at wall shear stresses ranging from 0.05 to 0.8 dyn/cm^2. As expected, higher E-selectin density supported a lower neutrophil rolling velocity at all wall shear stress levels tested (Fig. 4 *A*). Nevertheless, the rolling velocity curves at both E-selectin densities displayed a triphasic trend. At very low wall shear stresses, the rolling velocity increased with shear. In this same lower shear regime, the tether lifetime decreased as shear stress was increased (Fig. 3 *A*), typically associated with faster rolling behavior. In the middle range of wall shear stresses that correspond to the catch-bond region, the rolling velocity decreased with increasing shear stress. Finally, at higher wall shear stresses, the rolling velocity again increased with increasing force, which is the regime where slip bonds were observed again in tether lifetime experiments. Thus, the triphasic rolling velocity curve exhibits an inverse relationship with the triphasic tether lifetime curve, supporting our hypothesis that neutrophil rolling on E-selectin is governed by the slip-catch-slip bonds of E-selectin/ligand interaction.

In similarity to the tether lifetime curves, the triphasic changes in the rolling velocity curves were moderate and occurred in a narrow shear stress range. However, a comparison of the slopes of the two neighboring phases, as done for the tether lifetime data, revealed that the triphasic trend was significant, with $P < 0.05$ for both transitions from the low to intermediate and from the intermediate to high wall shear stresses, and for both site densities of E-selectin.

To ensure that the triphasic pattern of rolling velocity versus wall shear stress curve was due to molecular rather than cellular properties, we fixed neutrophils with 1% formaldehyde and measured their rolling velocity on E-selectin over the same range of wall shear stresses. The fixed neutrophils required a minimum of 250 μm^{-2} E-selectin for sufficient rolling to occur. Even at this high density, the fixed neutrophils rolled twice as fast as the unfixed neutrophils (Fig. 4 *B*). In addition, some cells skipped across the substrate, especially at higher shear stresses. Nevertheless, the average rolling velocity followed a statistically significant triphasic trend ($P = 0.009$ for the slope comparison of both transitions) over a range of wall shear stresses similar to that seen for unfixed neutrophils. This indicates that the triphasic velocity curve is a property of E-selectin binding and not a result of cellular features such as tether extrusions (33,34).

In addition to neutrophils, we also studied two other cell types that can roll on E-selectin: HL-60 and Colo-205. Colo-205 cells express the sLe^x isomer sLe^a (Fig. 1 *A*), which also binds to E-selectin (35). The average rolling velocity of HL-60 cells on 250 μm^{-2} E-selectin displayed a triphasic curve ($P < 0.0005$ for the slope comparison of both transitions) that is comparable to those of unfixed and fixed neutrophils (Fig. 5 *A*). For Colo-205 cells, the average rolling curve also exhibited a significant triphasic trend (Fig. 5 *B*), with $P < 0.0001$ and $P = 0.03$ for the slope comparisons of the transition from the low to intermediate and intermediate to high wall shear stresses, respectively.

DISCUSSION

Previous studies showed catch-slip bonds for P- and L-selectin interacting with PSGL-1 at forces in the range of 6–60 pN and 5–200 pN, respectively (11,12), and a potential slip bond preceding the catch-bond regime for E-selectin at low forces (19). Here, we demonstrate that E-selectin-mediated dissociation exhibits a triphasic trend, transitioning from slip bonds to catch bonds and then returning to slip bonds with increasing force. We observed triphasic curves in both the flow chamber and BFP experiments using neutrophil ligands and sLe^x.

The catch-bond regime measured by the BFP (Fig. 3 *C*) is narrower than that measured by the flow chamber (Fig. 3 *B*). Similar discrepancies were previously observed between

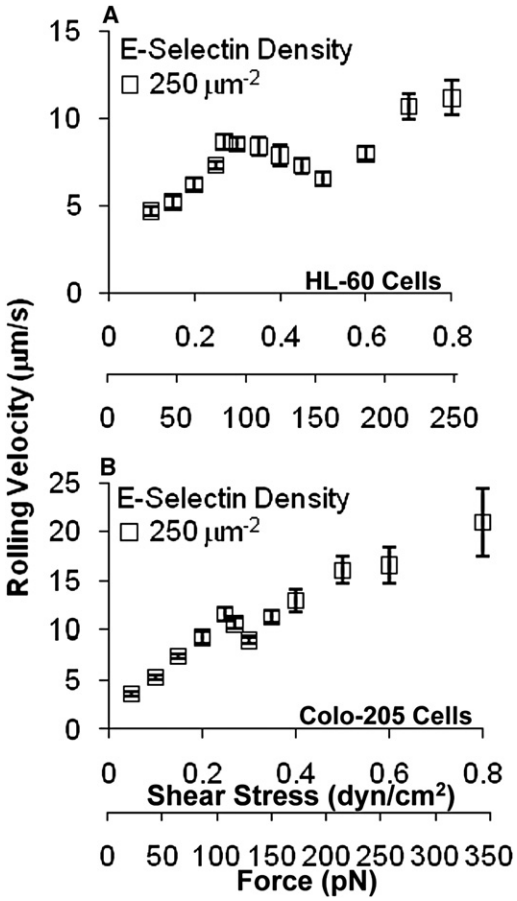

FIGURE 5 Triphasic shear stress dependence of tumor cell rolling velocities. (*A* and *B*) The velocities of HL-60 (*A*) and Colo-205 (*B*) cells rolling on 250 μm^{-2} E-selectin at various shear stresses. Data are presented as velocity mean ± SE of up to 25 cells.

force-dependent lifetimes measured by flow chamber and AFM (11,12,32) or BFP (23) for P-selectin (11) or L-selectin (12,23) or GPIbα (32) dissociating from their respective ligands. The reason for this is unclear; however, the BFP measured interactions in normal contact between two glass beads where E-selectin was coated by covalent coupling and sLe^x was coated by streptavidin capture, respectively. By comparison, the flow chamber measured binding in tangential contact between a sLe^x-bearing polystyrene bead and a coverglass where E-selectin was coated by adsorption. The differences in the E-selectin coating methods and their resulting molecular orientations, in the molecular contact, and in the loading rates of the two experiments may all impact the E-selectin/sLe^x dissociation kinetics. Despite the differences in the catch-bond regime, a triphasic trend for E-selectin-mediated dissociation was observed in both the flow chamber and BFP experiments.

In addition, the triphasic trend of the force-dependent lifetimes is supported by the force-dependent velocity measurements for cell rolling on E-selectin. The basis for this argument is a causal relationship between the bond lifetime of an interaction and the cell rolling velocity mediated by the interaction (36), i.e., the shorter the lifetimes, the faster the rolling velocity. This has been demonstrated for both L-selectin/ligands (13) and GPIbα/VWF (32) interactions. For the L-selectin/ligands and GPIbα/VWF cases, as force is increased, the cells roll more slowly in the catch-bond regime, where lifetimes are prolonged, and faster in the slip-bond regime, where lifetimes are shortened (13,32). For E-selectin, where three bond regimes exist, the force-dependent rolling velocity would be expected to have a triphasic curve, with the rolling velocity in each phase being inversely related to the tether lifetime. We observed such triphasic rolling velocities for unfixed and fixed neutrophils, HL-60 cells, and Colo-205 cells.

However, previous flow chamber (26) and AFM (37) studies did not observe the triphasic force-dependent off-rate of E-selectin/ligand dissociation. Since in the previous flow chamber experiments (26) tether lifetimes at only limited wall shear stress levels were measured over a wide range, the subtle triphasic trend might have been missed. In the previous AFM experiments (37), rupture force data were interpreted by dynamic force spectroscopy analysis based on the Bell model (10), which precluded catch bonds. Nevertheless, rigorous statistical analysis was required to demonstrate the significance of the slip-catch-slip transitions observed in this study. Small increments of shear stress that corresponded to small changes in tether lifetime metrics were tested to give higher resolution to the curve, and therefore resulted in high *P*-values for neighboring data points. Better proof of the triphasic pattern was found by comparing the slopes of the regression lines of each phase of the curve to determine whether they were statistically different. When we compared the trend line of the tether lifetime data in the slip-bond regimes with that of the catch-bond regime, we found that the slopes of the regression lines were significantly different, with the highest *P*-value being 0.04 for neutrophils. We then compared the catch-bond regime with the slip-bond regime in the high shear stress range, where fewer data points were collected due to our focus on the tether lifetimes in the catch-bond regime and forces below that. In the case of sLe^x-coated beads, where more tether lifetime data were collected in all regimes, the highest *P*-value was 0.004. Therefore, the transitions from monotonically increasing to decreasing and back to increasing trends in the triphasic curve were statistically significant. The same approach was used to test the triphasic pattern of the force-dependent rolling velocity curves. The transitions between any neighboring trends were also found to be statistically significant.

Because of the similarities among the three selectins in structure and function, our data provide a better understanding of the force-dependent dissociation kinetics for all selectins. The catch-slip transitional bonds previously shown for P- and L-selectin (11,12) were qualitatively similar to each other and to the latter two phases of the E-selectin

triphasic curves. However, the specificity of the different selectin-ligand interactions results in quantitative differences among their catch-slip bonds, which not only differ in their lifetime levels but also span different ranges of force. This difference allowed us to observe another slip-bond regime that precedes the catch-bond regime for E-selectin, whereas for P- and L-selectin the catch-bond regime extended into the lowest forces tested (11,12). Although bond lifetimes with P- and L-selectin were not observed at even lower forces, it seems reasonable to predict that their catch bonds would also transition back to slip bonds as force is further decreased. Not only would this be consistent with the structural and functional similarities of selectins, it would also agree with the zero-force lifetimes (reciprocal off-rates) measured at zero force by both two-dimensional (14–16) and three-dimensional (17,18) assays, which are much longer than the respective zero-force extrapolations of the lifetime versus force curves of the P-selectin (11) and L-selectin (12) with the catch-bond regime included.

With the slip-catch-slip bond transition for neutrophil ligand dissociation from E-selectin, the unstressed off-rate was determined to be $k^{\circ}_{\mathrm{off}} = 1.0\ \mathrm{s}^{-1}$ using a third-order polynomial. This agrees well with micropipette measurements of k°_{off} for HL-60 cells interacting with E-selectin, where $k^{\circ}_{\mathrm{off}} = 0.9\text{–}0.92\ \mathrm{s}^{-1}$ (15,38).

Physical models developed for biphasic catch-slip bonds (39) may need to be modified to account for triphasic slip-catch-slip bonds. Of interest, the sliding-rebinding model, which is based on molecular-dynamics simulations and explains the catch-slip bonds for ligand dissociation from P- and L-selectins (12,40) and GPIbα (32), also predicts a triphasic trend of the E-selectin/ligand bond lifetime curves (J. Lou and C. Zhu, unpublished data). Therefore, the sliding-rebinding model may describe the force-dependent ligand dissociation from all three selectins. In addition, the novel (to our knowledge) observation presented here highlights the need for further studies to investigate the physiological role of the triphasic force-dependent dissociation of E-selectin/ligand bonds.

SUPPORTING MATERIAL

Three figures are available at http://www.biophysj.org/biophysj/supplemental/S0006-3495(10)00714-9.

The authors thank Tadayuki Yago for performing site density measurements and providing advice on the flow chamber experiments.

This work was supported by grants AI44902, HL090923, and AI077343 from the National Institutes of Health; HL65631, a National Institutes of Health Research Supplement for Underrepresented Minorities; and a National Science Foundation predoctoral fellowship.

REFERENCES

1. Frenette, P. S., S. Subbarao, …, D. D. Wagner. 1998. Endothelial selectins and vascular cell adhesion molecule-1 promote hematopoietic progenitor homing to bone marrow. *Proc. Natl. Acad. Sci. USA.* 95:14423–14428.
2. Mazo, I. B., J. C. Gutierrez-Ramos, …, U. H. von Andrian. 1998. Hematopoietic progenitor cell rolling in bone marrow microvessels: parallel contributions by endothelial selectins and vascular cell adhesion molecule 1. *J. Exp. Med.* 188:465–474.
3. Springer, T. A. 1994. Traffic signals for lymphocyte recirculation and leukocyte emigration: the multistep paradigm. *Cell.* 76:301–314.
4. McEver, R. P., K. L. Moore, and R. D. Cummings. 1995. Leukocyte trafficking mediated by selectin-carbohydrate interactions. *J. Biol. Chem.* 270:11025–11028.
5. Foxall, C., S. R. Watson, …, B. K. Brandley. 1992. The three members of the selectin receptor family recognize a common carbohydrate epitope, the sialyl Lewis(x) oligosaccharide. *J. Cell Biol.* 117:895–902.
6. Phillips, M. L., E. Nudelman, …, J. C. Paulson. 1990. ELAM-1 mediates cell adhesion by recognition of a carbohydrate ligand, sialyl-Lex. *Science.* 250:1130–1132.
7. Polley, M. J., M. L. Phillips, …, J. C. Paulson. 1991. CD62 and endothelial cell-leukocyte adhesion molecule 1 (ELAM-1) recognize the same carbohydrate ligand, sialyl-Lewis x. *Proc. Natl. Acad. Sci. USA.* 88:6224–6228.
8. Zhou, Q., K. L. Moore, …, R. D. Cummings. 1991. The selectin GMP-140 binds to sialylated, fucosylated lactosaminoglycans on both myeloid and nonmyeloid cells. *J. Cell Biol.* 115:557–564.
9. McEver, R. P. 2002. Selectins: lectins that initiate cell adhesion under flow. *Curr. Opin. Cell Biol.* 14:581–586.
10. Bell, G. I. 1978. Models for the specific adhesion of cells to cells. *Science.* 200:618–627.
11. Marshall, B. T., M. Long, …, C. Zhu. 2003. Direct observation of catch bonds involving cell-adhesion molecules. *Nature.* 423:190–193.
12. Sarangapani, K. K., T. Yago, …, C. Zhu. 2004. Low force decelerates L-selectin dissociation from P-selectin glycoprotein ligand-1 and endoglycan. *J. Biol. Chem.* 279:2291–2298.
13. Yago, T., J. Wu, …, R. P. McEver. 2004. Catch bonds govern adhesion through L-selectin at threshold shear. *J. Cell Biol.* 166:913–923.
14. Zhu, C., M. Long, …, P. Bongrand. 2002. Measuring receptor/ligand interaction at the single-bond level: experimental and interpretative issues. *Ann. Biomed. Eng.* 30:305–314.
15. Huang, J., J. Chen, …, M. Long. 2004. Quantifying the effects of molecular orientation and length on two-dimensional receptor-ligand binding kinetics. *J. Biol. Chem.* 279:44915–44923.
16. Chen, W., E. A. Evans, …, C. Zhu. 2008. Monitoring receptor-ligand interactions between surfaces by thermal fluctuations. *Biophys. J.* 94:694–701.
17. Mehta, P., R. D. Cummings, and R. P. McEver. 1998. Affinity and kinetic analysis of P-selectin binding to P-selectin glycoprotein ligand-1. *J. Biol. Chem.* 273:32506–32513.
18. Nicholson, M. W., A. N. Barclay, …, P. A. van der Merwe. 1998. Affinity and kinetic analysis of L-selectin (CD62L) binding to glycosylation-dependent cell-adhesion molecule-1. *J. Biol. Chem.* 273:763–770.
19. Piper, J. W. 1997. Force dependence of cell bound E-selectin/carbohydrate ligand binding characteristics. Ph.D. thesis. School of Mechanical Engineering, Georgia Institute of Technology, Atlanta, GA.
20. Xia, L., J. M. McDaniel, …, R. P. McEver. 2004. Surface fucosylation of human cord blood cells augments binding to P-selectin and E-selectin and enhances engraftment in bone marrow. *Blood.* 104:3091–3096.
21. Patel, K. D., K. L. Moore, …, R. P. McEver. 1995. Neutrophils use both shared and distinct mechanisms to adhere to selectins under static and flow conditions. *J. Clin. Invest.* 96:1887–1896.
22. Zimmerman, G. A., T. M. McIntyre, and S. M. Prescott. 1985. Thrombin stimulates the adherence of neutrophils to human endothelial cells in vitro. *J. Clin. Invest.* 76:2235–2246.
23. Lou, J., T. Yago, …, R. P. McEver. 2006. Flow-enhanced adhesion regulated by a selectin interdomain hinge. *J. Cell Biol.* 174:1107–1117.

24. Smith, M. J., E. L. Berg, and M. B. Lawrence. 1999. A direct comparison of selectin-mediated transient, adhesive events using high temporal resolution. *Biophys. J.* 77:3371–3383.

25. Ushiyama, S., T. M. Laue, …, R. P. McEver. 1993. Structural and functional characterization of monomeric soluble P-selectin and comparison with membrane P-selectin. *J. Biol. Chem.* 268:15229–15237.

26. Alon, R., S. Chen, …, T. A. Springer. 1997. The kinetics of L-selectin tethers and the mechanics of selectin-mediated rolling. *J. Cell Biol.* 138:1169–1180.

27. Yago, T., A. Leppänen, …, R. P. McEver. 2002. Distinct molecular and cellular contributions to stabilizing selectin-mediated rolling under flow. *J. Cell Biol.* 158:787–799.

28. Goldman, A. J., R. G. Cox, and H. Brenner. 1967. Slow viscous motion of a sphere parallel to a plane wall. II. Couette flow. *Chem. Eng. Sci.* 22:653–660.

29. Chen, W., V. I. Zarnitsyna, …, C. Zhu. 2008. Measuring receptor-ligand binding kinetics on cell surfaces: from adhesion frequency to thermal fluctuation methods. *Cell Mol. Bioeng.* 1:276–288.

30. Evans, E., V. Heinrich, …, K. Kinoshita. 2005. Nano- to microscale dynamics of P-selectin detachment from leukocyte interfaces. I. Membrane separation from the cytoskeleton. *Biophys. J.* 88: 2288–2298.

31. Zar, J. 1974. Biostatistical Analysis. Prentice-Hall, Englewood Cliffs, NJ.

32. Yago, T., J. Lou, …, C. Zhu. 2008. Platelet glycoprotein Ibα forms catch bonds with human WT vWF but not with type 2B von Willebrand disease vWF. *J. Clin. Invest.* 118:3195–3207.

33. Schmidtke, D. W., and S. L. Diamond. 2000. Direct observation of membrane tethers formed during neutrophil attachment to platelets or P-selectin under physiological flow. *J. Cell Biol.* 149:719–730.

34. Ramachandran, V., M. Williams, …, R. P. McEver. 2004. Dynamic alterations of membrane tethers stabilize leukocyte rolling on P-selectin. *Proc. Natl. Acad. Sci. USA.* 101:13519–13524.

35. Zhang, K., D. Baeckström, and G. C. Hansson. 1994. A secreted mucin carrying sialyl-Lewis a from colon carcinoma cells binds to E-selectin and inhibits HL-60 cell adhesion. *Int. J. Cancer.* 59:823–829.

36. Zhu, C., T. Yago, …, R. P. McEver. 2008. Mechanisms for flow-enhanced cell adhesion. *Ann. Biomed. Eng.* 36:604–621.

37. Zhang, X., D. F. Bogorin, and V. T. Moy. 2004. Molecular basis of the dynamic strength of the sialyl Lewis X—selectin interaction. *ChemPhysChem.* 5:175–182.

38. Long, M., H. Zhao, …, C. Zhu. 2001. Kinetic measurements of cell surface E-selectin/carbohydrate ligand interactions. *Ann. Biomed. Eng.* 29:935–946.

39. Prezhdo, O. V., and Y. V. Pereverzev. 2009. Theoretical aspects of the biological catch bond. *Acc. Chem. Res.* 42:693–703.

40. Lou, J., and C. Zhu. 2007. A structure-based sliding-rebinding mechanism for catch bonds. *Biophys. J.* 92:1471–1485.